Faraday Discussions

Cite this: *Faraday Discuss.*, 2026, **262**, 327

PAPER

Improved 2PP additive manufacturing build/process quality *via* the use of hyperbranched pre-polymer

Andrea A. Konta,[a] Michelle Duong,[b] Joseph Sefton,[ab] Valentina Cuzzucoli Crucitti,[a] Amy Stimpson,[a] Sophie Goodwin,[a] Thomas Swift,[c] Gustavo F. Trindade,[a] Yinfeng He,[a] Mohamed Adam,[b] Eleanor Binner,[b] Laura Ruiz Cantu,[a] Cameron Alexander,[d] Ricky D. Wildman[ab] and Derek J. Irvine *[ab]

Received 7th June 2025, Accepted 29th July 2025
DOI: 10.1039/d5fd00097a

This study reports the first systematic study investigating the potential of using hyperbranched (HB) polymers as novel materials for improving two photon polymerisation (2PP) processing. It demonstrated that HB polymer containing additive manufacturing resins can be successfully formulated and used to print: (a) mono-/multi-material structures, the latter containing monomers of different functionality (*i.e.*, hydrophilic/hydrophobic mixes), (b) with a broader range of printing conditions, (c) to high levels of cure and (d) at faster processing speeds than monomeric resins. A printed multi-material structure was confirmed to contain both feed materials and exhibit high cure by ToF-SIMS and Raman analysis, respectively. Thus, HB polymers were shown to improve mixing in multi-functional resins and overcome 2PP chemistry restrictions. When processing with selected HB polymers, both the polymerisation "onset" and "burning" thresholds were improved compared to monomeric resins. Processing more reactive HB polymers still increased the overall processing window compared to the 2PP processing of the equivalent monomer, but the "burning" threshold was in fact lowered, which was linked to depolymerisation events. Thus, a HB polymer was subject to degradation studies and shown to produced more residual material (*i.e.* "char") than linear materials, which delivers the decolourisation in 2PP "burning". This study confirms that using HB polymers can extend the viability and utility of 2PP processing, improvements that were delivered by understanding the reactivity of these pre-polymers toward both polymerisation and depolymerisation.

[a]*Centre for Additive Manufacturing, Faculty of Engineering, University of Nottingham, Nottingham, NG7 2RD, UK. E-mail: derek.irvine@nottingham.ac.uk*

[b]*Department of Chemical and Environmental Engineering, Faculty of Engineering, University of Nottingham, Nottingham, NG7 2RD, UK*

[c]*School of Chemistry and Biosciences, University of Bradford, Bradford, BD7 1DP, UK*

[d]*School of Pharmacy, Faculty of Science, University of Nottingham, Nottingham, NG7 2RD, UK*

Introduction

Additive manufacturing (AM), often referred to as 3D printing, encompasses a series of processes that build structures *via* multiple deposition and/or energy application events.[1] Several of these have the capability to transform a computer-aided design, through a standard tessellation language (STL) file, directly into a physical structure.[2] In the area of AM with polymeric materials, one key challenge of AM processing is to ensure that high levels of monomer cure and crosslinking are achieved to produce a robust device.[3,4] This is important to ensure that the material properties of an AM processed device do not alter with time and/or no leachate of organic monomer is introduced into the media/system/anatomy that surrounds it.[5] However over crosslinking the system can/will introduce brittleness.[6] Thus, controlling the level of monomer version and branching density that is inherent in the materials of construction of an AM device is of critical importance to successfully producing a 3D printed device.[7]

In recent years, there has been an increasing interest in using AM techniques to fabricate three-dimensional (3D) devices with complex microstructures for many application areas, including biomedical and photonics.[8,9] However, obtaining very high levels of build detail has been found to be a significant challenge.[10,11] In recent years, two-photon polymerisation (2PP) has been shown to be one of the preeminent methods for producing well-defined 3D micro/nano structures.[12–15] This technique fabricates devices *via* a point-by-point strategy, using a photosensitive resin and a femtosecond infrared (IR) laser.[16,17] The initiator components within the resin absorb two photons in the near IR spectrum and initiate the polymerisation by triggering a photochemical reaction in a specific focused region, referred to as a voxel.[18] The overall build size can be scaled up to the centimetre range with adaptable voxel size and hydrogels, nanomaterials and biomaterials can be processed with this approach.[19]

To successfully apply 2PP, it is essential to understand a system's printing parameters which, in many respects, are dependent upon the functional properties of the resin. In practice, 2PP has an operating window which allows successful production of the desired target structures, where typically a tuneable femtosecond laser (operating in a working range 690–1040 nm; pulse width of 140 fs, and pulse repetition rate of 80 MHz) is the excitation source.[20] At low laser powers, insufficient energy is absorbed to sustain full polymerization, which will not lead to structures with nanoscale fidelity. However, the application of excessive laser power results in damaged structures caused by localized "burning" of the resin, *i.e.* formation of damaged and discoloured structures currently attributed to "boiling" of the monomer.[19] Both effects have been attributed to the level of laser power exposure each unit of the structure receives. There are several processing characteristics that can control/limit the effective laser power exposure and so define 2PP's printing window, *i.e.* scan speed and/or hatching distance.[19]

The processing window for 2PP depends on the resin formulation. There have been studies of various monomer and photo-initiator combinations to try to maximise the spread of processing conditions that can be applied in 2PP.[20] However, there is potentially more to the concept of "burning" 2PP structures than simply "boiling" the monomers within the resin. The resin materials, because the polymerisation process is exothermic, may also become involved in

rapid thermally induced polymerisation/depolymerisation processes triggered by the laser energy. Thus, one potential method to increase the operational window from a polymerisation perspective is to introduce pre-polymer into the resin to reduce the amount of reaction that is required during the build, so reducing the level of reaction based exotherm it experiences.

When introducing prepolymers into a 2PP resin, one important characteristic that determines the resin's suitability is that the components must exhibit good molecular mobility, *i.e.* all the monomers/pre-polymers have sufficient molecular freedom to participate in the polymerization process. Typically, this requires a resin to exhibit specific viscosity characteristics.[20,21] Consequently, polymeric additives suitable for printing often have low glass transition temperatures (T_g), as these materials exhibit greater inter-chain mobility.[22] The viscosity an oligomer/polymer exhibits is also influenced by its molecular weight and chain entanglement, with those with higher molecular weights and/or exhibiting more chain entanglement tending to possess higher viscosities.[23] Thus, materials with low viscosities can be produced as oligomers (low molecular weight polymers) or branched polymers, such as multi-arm stars and hyperbranched (HB) polymers.[23] The former properties are typically related to their low molecular weight, whilst the latter cannot chain pack/entangle efficiently as they exhibit what is referred to as a "globular" molecular structure.[24,25] Consequently, introducing branching allows materials with high molecular weights to be produced that still show significantly lower viscosities compared to the comparative linear materials *i.e.* single chains containing similar monomer pendant group functionalities. Consequently, they have been applied to control the viscosity during processing in fields like additives,[24,26] coatings,[26] or inkjet printing inks.[26–29]

HB polymers are also of potential advantage in 2PP processing because their synthesis involves the use of multi-functional monomers, *i.e.* monomers containing several polymerisable moieties, to enable the generation of multi-functional macromonomers.[30–32] Thus, an additional positive characteristic of HB polymers is that they can retain a sufficient quantity of photoreactive functional groups within their molecular structure to potentially ensure 2PP curing times/levels are maintained or increased, if compared to when linear molecules are added to resin formulations.[23] This hypothesis has been supported by literature reports of the investigation of adding HB materials to ink-jetting resins, which resulted in faster curing than with linear counterpart additives.[28,29] It has also been reported that increasing chain branching above a critical value avoided polymer degradation during printing, which was attributed to the polymer architecture maintaining its conformation so that it was not affected by the constriction on the flow as it passes through the print head.[27,29] However, there are few reports of these materials being used in Vat photo-polymerisation AM/2PP techniques. Ning *et al.* reported the use of HB polysiloxane to modify epoxy resins for stereolithography 3D printing,[33] where this study showed that the HB polysiloxane addition to the epoxy resin at different concentrations improved the heat resistance of the resin. It also had an effect on the mechanical properties of the structures, with resins containing a 5 wt% loading of HB material shown to exhibit significant increases in the toughness of the printed structures.[33] However, this increased reactivity and resistance to degradation may also play a part in the "burning" behaviour observed in 2PP polymerisation, which still needs to be investigated.

Thus, this study explored the addition of novel HB polymers to 2PP resins to define their potential to: (a) expand the technique's processing window, (b) increase the library of the materials available for 2PP printing, (c) enable multi-material printing (*i.e.* printing with two monomers that possess different material properties *e.g.* hydrophobic and hydrophilic) and (d) explore their degradation properties to improve understanding of the "burning" process. To achieve this, HB materials were synthesised *via* conventional thermal polymerisation and formulated into resins for both mono- and multi-material 2PP printing. Target structures were then manufactured with two optimised resins, whilst a HB polymer was subjected to high temperature degradation to elucidate how their depolymerisation characteristics may contribute to the "burning" effect. The 2PP material from these structures was subjected to Raman, SEM and ToF-SIMS analysis and the data compared to that of linear counterparts to determine cure levels and that successful multi-material printing had been achieved.

Experimental

Materials

Poly(ethylene glycol)diacrylate (PEGDA) (250 g mol^{-1}), tricyclo[5.2.1.$0^{2,6}$]decanedimethanol diacrylate (TCDMDA), methyl methacrylate (MMA), ethylene glycol dimethacrylate (EGDMA), 2-benzyl-2-(dimethylamino)-1-[4-(4-morpholinyl)phenyl]-1-butanone (Irgacure 369, photoinitiator), 3-mercaptopropionic acid (3-MPA, chain transfer agent), and propylene glycol methyl ether acetate (PGMEA) were obtained from Sigma Aldrich, Inc (UK). 2,2′-Azobis(2-methylpropionitrile) (AIBN, thermal initiator) was acquired from Fluorochem Ltd (UK). Bis[(difluoroboryl)diphenylglyoximato]cobalt(II) (PhCoBF, chain transfer agent) was purchased from DuPont (Wilmington, DE, USA). Externally sourced commercially obtained PMMA polymer cast sheet products were sourced by Mitsubishi Chemicals UK (Redcar, UK). Isopropanol, toluene and hexane were acquired from Fisher Scientific Ltd (UK). All materials were used as received without further purification.

General synthetic procedure of the hyperbranched polymers

Note on gelation. This was defined as the point where the solution ceased to be a free-flowing, easily stirred liquid and became a rubbery solid and was readily observable visually as the solution was unable to be stirred magnetically. This was confirmed by withdrawing a sample of the reaction mixture and attempting to dilute it in chloroform. If gelation had occurred, the sample was non-dissolvable, and the time taken for this was defined as the gelation time. It represents a change from an HB system to an extended, 3D, cross-linked system.

General synthetic procedure of the hyperbranched polymers for degradation studies. Copolymers were produced *via* the CCTP controlled reaction of MMA and EGDMA to give a 95 : 05 mol% or 65 : 35 mol% ratio of the monomers respectively, see quantities used in Table 1 for the smaller scale "scouting" experiments. The materials tested in the TGA, and thermal degradation studies were scaled by 20 times these quantities.

The desired quantities of these monomers, initiator, solvent and control agent were introduced into a Schlenk flask equipped with a magnetic stirrer bar and containing an inert nitrogen atmosphere. Bis[(difluoroboryl)diphenylglyoximato]

Table 1 Quantities of reagents used in CCTP HB polymer synthesis procedures

MMA : EGDMA ratio	95 : 05 mol%	65 : 35 mol%
MMA	5 mL (46.74 mmol)	5 mL (46.74 mmol)
EGDMA	0.5 mL (2.65 mmol)	5 mL (26.51 mmol)
PhCoBF	0.147 mg (0.0002 mmol)	1.021 mg (0.0015 mmol)
Toluene (monomer : solvent)	1 : 2 (v/v%)[a]	1 : 1 (v/v%)[a]
AIBN	0.5 mol%	1.5 mol%

[a] Solvent increased for 95 : 5 mol% HB polymer to increase "time to gelation" and improve conversion.

cobalt(II) and AIBN were then added to the flask under a nitrogen atmosphere. Different levels of PhCoBF were used to ensure that the gelation occurred over a timescale that allowed the reaction to be terminated prior to its gel point. In the case of the higher crosslinker ratios this entailed increasing the PhCoBF ratio. The vial was degassed for 1 h using nitrogen and then the reaction vessel was immersed in a preheated oil bath which was thermostatically controlled to remain at 80 °C. An initial "scouting" reaction was conducted which was reacted until gelation occurred, at which point the time was noted A repeat reaction was then conducted which was quenched ~5 minutes before the time gelation was known to occur in the initial "scouting" experiment. Once cooled, the solution was added dropwise to cold (0 °C) methanol. The resulting precipitate was collected *via* filtration to provide a colourless brown/white solid, which was then dried to constant mass under vacuum (colouration due to residual PhCoBF).

General synthetic procedure of the hyperbranched polymers for 2PP printing. The di-functional TCDMDA or PEGDA monomer (1 mL), toluene solvent (2 mL), 3-MPA control agent (from 5 to 65 mol% dependent on the specific experiment) and AIBN initiator (between 0.1 to 3 wt%, dependent on the specific experiment) were all added to a reaction vessel. The mixture was degassed with argon for 30 min, then immersed in a pre-heated oil bath at 65 °C and reacted for the set number of minutes defined to terminate the reaction prior to the gel point from the "scouting" experiments. The polymerisation was quenched *via* oxygen ingress and immersion in an ice bath to prevent further crosslinking that would result in the formation of a gel. The polymer (HBpPEGDA or HBpTCDMDA) was isolated *via* dropwise precipitation into cold (0 °C) hexane antisolvent. To isolate the materials, the supernatant was decanted, and the viscous product was allowed to dry to constant mass under vacuum.

General method for thermal degradation of HB polymers. A conventional pyrolysis system was utilised to conduct the thermal degradation studies, see Fig. S1 and Description S1 for an image and detail of the apparatus organisation. The furnace was set to 70% output power and 450 °C or 700 °C using the built-in controller as outlined by the user manual. The heater thermostat was adjusted accordingly to heat the overheads to within the range of 120–160 °C to ensure distillation. Once the overheads reached the target temperature, the furnace heating was begun and the sample pyrolyzed until no further pyrolytic vapours were generated. Then the furnace and heating tape were switched off and the reactor tube cooled to <40 °C before handling. Once cooled, the quartz reactor was weighed, and the solid yield calculated.

Characterization of standard thermally polymerised hyperbranched polymers

Proton nuclear magnetic resonance analysis. ^{1}H NMR was performed on a Bruker AV400 spectrometer (400 MHz) at 25 °C. Samples were prepared as 10 mg mL^{-1} solutions in deuterated chloroform ($CDCl_3$) to which chemical shifts, measured in δ_H (ppm), were referenced to (residual $CHCl_3$ at 7.26 ppm). Analysis of spectra used Mestrelab Mnova 10.0 software.

Gel permeation chromatographic analysis. GPC was performed on an Agilent 1260 Infinity system (Agilent Technologies, USA) equipped with a PL-gel 5 mm guard column and two PL-gel mixed-C (7.5 mm × 300 mm) columns in series. Tetrahydrofuran (THF, HPLC grade, Fisher Scientific) was the mobile phase at a flow rate of 1 mL min^{-1}. A Wyatt Optilab light scattering detector and a differential refractometer (DRI) were used for sample detection and analysis. The differential index of refraction value (dn/dc), 0.0816, was used to calculate the polymer molecular weight and dispersity. GPC samples were made up as 2 mg mL^{-1} solutions in HPLC grade THF which were filtered into a sample vial through a syringe filter (Whatman, 25 mm, 0.2 mm). Analysis of the spectra obtained was carried out using Astra software.

Thermogravimetric analysis. TGA was performed on a TA instruments Discovery Q500. All samples were ground into powder form and loaded into instrument pans. The instrument was programmed to run through 50–700 °C at 10 °C min^{-1} under 60 mL min^{-1} of nitrogen flow.

DOSY NMR of HB polymers. Diffusion measurements were performed on a Bruker Avance Neo spectrometer (600 MHz) equipped with a Bruker diffBB probe. Samples were dissolved in deuterated chloroform (1 mg mL^{-1}) and 400 mL was loaded into the instrument in 5 mm OD borosilicate tubes. The Branching Density (Degree of Branching) was determined from δ_H integrals measured under these conditions, with 4.4 ppm ($C\mathbf{H_2}C\mathbf{H_2}$ – crosslinker), 3.6 ppm ($OC\mathbf{H_3}$ – monomer), 6.3 ppm (C═C**H**H – unsaturated chain ends). Eqn (1) was used to determine branching density:

$$\text{Branching density} = \frac{[1\text{H crosslinker}]}{[1\text{H crosslinker}] + [1\text{H monomer}] + [1\text{H chain end}]} \quad (1)$$

Samples were then analysed using a DOSY pulse sequence with 64 gradient steps (γ: 26 752 rad s^{-1} Gauss^{-1}, δ 0.0036 S, Δ 0.0599 S). The instrument was controlled using Topspin V4.1.1 equipped with the Bruker Dynamic Centre module for data analysis. Analyte and solvent diffusions were analysed using the following δ_H peaks: 7.3 ppm ($CDCl_3$, used to provide sample viscosity correction factor), 6.2, 4.4, 3.6, 1.8 ppm (all peaks arising from the polymer analyte) and 2.4 ppm (peaks suspected to present residual trace toluene). The hydrodynamic radii of the polymer coils were determined using the Stokes–Einstein equation with analyte viscosity correction applied compared to a $CDCl_3$ standard analysed under equivalent conditions.

Formulation of 2PP resins containing HB polymers for printing

Copolymer formulations (*i.e.* HB material plus a difunctional monomer) for the 2PP system were prepared by mixing precalculated target concentrations of the required monomers in a 5 mL amber vial in a UV-free environment. A pre-weighed quantity of the selected initiator (Irgacure 369), such that it was between 0.1 to

3 wt% of total solution, dependent on the specific experiment, was then added to the vial. The vial was then agitated on a hotplate at 60 °C for 1 h. Formulations containing only HB materials were prepared by adding the polymers to the vial, followed by the photoinitiator, and the vial was agitated for 30 min at room temperature. Copolymer formulations containing both HB polymer and linear monomers were prepared by adding the materials to the amber vial and mixing them at low stirring on a hotplate for 20 min. Once well mixed, photoinitiator was added to the vial and the formulation was left stirring for another 30 min at room temperature.

2PP manufacturing window determination with the formulated resins

Methacrylate functionalization of glass coverslips. Glass coverslips (22 mm × 22 mm) were activated using O_2 plasma (p_i = 0.3 mbar, 100 W, 5 min) and immediately transferred into dry (4 Å MS) toluene (50 mL) under argon. 3-(Trimethoxysilyl)propyl methacrylate (1 mL) was added, and the reaction mixture heated to 50 °C for 24 h. The slides were then cooled to room temperature and washed with 3 × 10 mL fresh toluene using sonication. The slides were then dried under vacuum in a silicone-free vacuum oven (50 °C) for 24 h.

Manufacturing structures by 2PP printing. Structures were printed with a commercial two-photon system (Nanoscribe Photonic Professional GT) using a 780 nm wavelength fibre laser, an 80 MHz pulse frequency, and a pulse duration of 120 fs. The laser beam was focused with an oil immersion objective (63×, Numerical Aperture (NA) = 1.4). Specimens were manufactured by moving the laser beam in the *X*–*Y* direction with mirrors and by moving the piezo stage in the *Z* direction (printing in galvo-mode). The treated glass coverslips were the substrate used to print on. The coverslips were mounted on the sample holder with tape. A drop of oil was added to the bottom of the slide and a drop of the formulation was added to the top of the slide. The sample holder with the coverslips was then put into the printer to allow manufacturing. The structures were designed on AutoCAD software. To eliminate unpolymerized material from the final printed structures, samples were immersed in propylene glycol monomethyl ether acetate (PGMEA) for 6 to 24 h. After this, structures were thoroughly washed in isopropanol for 10 min to eliminate any residual PGMEA and air-dried.

Evaluation of feasible polymerization window. The window of 2PP printing conditions that delivered adequate manufacturing of the target structure and resin crosslinking was determined by testing the 2PP resins *via* printing target structures at different laser powers and scan speeds. This step allowed to determine the "onset" threshold and burning threshold of the different resins being evaluated. The combination of parameters that allowed for successful manufacturing were confirmed by scanning electron microscopy (SEM).

Printed sample characterization

Scanning electron microscopy. SEM was performed using a Hitachi TM3030 table-top SEM. The images were obtained using a 15 keV acceleration voltage with the composition (COMPO) imaging mode. The samples were previously coated with gold before SEM imaging.

Raman spectroscopy. Raman spectroscopy was conducted using a Horiba Jobin Yvon LabRAM HR equipped with an automated *xyz* stage (Märzhäuser).

Excitation was provided by a laser line at $\lambda = 785$ nm ($P = 24$ mW). A 100× objective lens and a confocal pinhole of 50 μm were used. To simultaneously scan a range of Raman shifts, a 600 lines mm^{-1} rotatable diffraction grating along a path length of 800 mm was employed. Spectra were acquired using a Synapse CCD detector (1024 pixels) thermoelectrically cooled to −60 °C. Before spectra collection, the instrument was calibrated using the zero-order line at 0 nm and a standard Si(100) reference band at 520.7 cm^{-1}. For single point measurements, spectra were acquired over the range 600–1850 cm^{-1} with an acquisition time of 60 to 120 seconds and 4 accumulations. The spectral resolution is 0.6 cm^{-1} for the 785 nm laser. The spatial resolution is ~1 μm and ~3 μm in the lateral (xy) and axial (z) directions respectively. Spectra were baseline-corrected using a fourth-order polynomial fitting model. The amount of Reacted Vinyl Group (RVG) was calculated using the following equation:

$$\mathrm{RVG} = 1 - \frac{A_{C=C}/A_{C=O}}{A'_{C=C}/A'_{C=O}} \quad (2)$$

where $A_{C=C}/A_{C=O}$ is the area under the peaks in polymerized structures and $A'_{C=C}/A'_{C=O}$ is the peak area of unpolymerised formulation. Samples were post processed before analysis by submerging them in PGMEA solvent for 24 h, then rinsing in IPA for 10 min and air-drying.

Time of flight secondary ion mass spectroscopy. ToF-SIMS of positively charged secondary ions was conducted using a TOF-SIMS IV system from IONTOF GmbH (Münster, Germany) using a 25 keV Bi^{3+} ion beam in burst-alignment, which provides high spatial resolution while compromising mass resolution to unit mass, and a low-energy (20 eV) electron flood gun employed to neutralise charge build-up. Secondary ion maps were acquired by raster scanning the primary ion beam over areas up to 150 × 150 μm^2. 3D depth profiling of the samples was carried out in dual-beam mode with the 25 keV Bi^{3+} primary ion beam in burst alignment mode (high spatial resolution) and a 210 × 210 μm^2 sputter crater formed using a 10 keV argon GCIB delivering 5 nA. The analysis was performed in the "non-interlaced" mode with one sputter frame and a single analysis scan per cycle and a pause time in between cycles of 0.5 s. The ToF analyser was set with 200 μs cycle time, resulting in a mass range between 0 and 3400 mass units. Data for depth profiles was reconstructed from the centre 50 × 50 μm^2 of the printed sample. The depth scale was estimated based on the sputter yield of known reference organic materials.[34]

Results and discussion

Three HB polymers, HB poly(ethylene glycol)diacrylate (HBpPEGDA), HB poly(-tricyclo[5.2.1.0^{2,6}]decanedimethanol diacrylate) (HBpTCDMDA) and HB poly(-methyl methacrylate-*co*-ethylene glycol dimethylacrylate) (HBpMMA-*co*-EGDMA) were synthesised *via* conventional thermal polymerisation (see monomer molecular structures in Scheme S1). The first two were utilised in 2PP processing, to define their influence on the process. The last was subject to TGA and high temperature degradation analysis to compare HB degradation characteristics with linear PMMA materials, whose degradation has been extensively investigated.[35–39] Chain transfer mediated free radical techniques were used to

control the HB polymerisation, where either 3-mercaptopropionic acid (3MPA) or bis[(difluoroboryl)diphenylglyoximato]cobalt (PhCoBF) were the chain transfer agents (CTA) used to delay the onset of gelation and allow the formation of HB polymers. For HBpTCMDMA and HBpPEGDA, which are acrylates, 3MPA was used to maximise yield, while PhCoBF was used with the methacrylate monomers to generate HBpMMA-*co*-EGDMA due to its very high chain transfer constant with methacrylates and because it doesn't introduce a sulphur moiety, that may produce noxious species during the high temperature treatment.[40]

To investigate the gelation characteristics of these polymerisations, different concentrations of AIBN, from 0.1% to 3% wt with respect to monomer, were used to initiate polymerisations and the time to gel formation, *i.e.* the onset of an insoluble 3D network formation, was measured for each concentration. For all polymers, the lowest concentration exhibited the longest gel point time and the highest the shortest (see Table S1). For example, the gel point for HBpTCMDMA at 0.1 wt% was found to be 31 minutes, whilst at 3 wt% it was significantly shorter at 4 min. As the same trend was observed with other monomers, the optimal AIBN concentration for subsequent polymerisations was set at 0.1 wt%. Secondly, the concentration of 3MPA was varied from 5–65 mol% to determine the effect this had on gel time of a HBpTCMDMA polymerisation, and the results showed no significant difference in gel point across all CTA concentrations (Fig. S2). To isolate the target solvent soluble HB polymers, this TCDMDA reaction was repeated and quenched after 25 min and the polymer isolated *via* precipitation and drying. Following the success of this screening with TCDMDA, HBpPEGDA and HBpMMA-*co*-EGDMA were generated, and a summary of the resultant polymers' chemical properties is shown in Table 2.

Inspection of the characterisation in Table 2, showed broad $Đ$ values for all the HB polymers, indicating that branching had occurred. The yields were above 50%, indicating that conversion was at a scale that would allow further printing/property evaluation. HBpPEGDA was noted to have a higher yield, suggesting that the more flexible structure/lower "T_g" of this monomer/polymer allows for a more efficient/rapid branching process compared to HBpTCMDMA and HBpMMA-*co*-EGDMA. This also suggested that comparison of the M_w values for these polymers should be regarded as relatively speculative, due the effects on the hydrodynamic volume of the HB polymer's "globular" structure and the relative rigidity of the monomer's molecular structures. In practice, it can only be inferred that a branched structure has successfully been synthesised.

Table 2 Yield and GPC chromatographic data for the products of HB polymerisations conducted at 65 °C (entries 1 and 2) and 80 °C (entry 3), using 0.1 wt% (entries 1 and 2) or 0.5 wt% (entries 3 and 4) AIBN and 3MPA (entries 1 and 2) or PhCoBF (entries 3 and 4) as CTA

Entry	Polymer	Co-monomer ratio MMA : EGDMA (mol%)	Yield[a] (%)	M_w[b] (g mol^{-1})	$Đ$[b]
1	HBpTCMDMA	—	60	13 000	3.9
2	HBpPEGDA	—	81	190 000	6.6
3	HBpMMA-*co*-EGDMA	95 : 05	62	41 000	4.6
4	HBpMMA-*co*-EGDMA	65 : 35	61	25 000	3.1

[a] Obtained gravimetrically. [b] Determined by GPC.

To investigate the advantage/suitability of HB polymers in 2PP, when compared to benchmark linear multi-reactive group monomers, formulations were prepared with the following components: (a) HB polymers alone, (b) a mix of HB polymers and multi-reactive monomers, and (c) multi-reactive monomers alone (formulations in Table S2). These were 2PP printed to screen their printing windows by applying different laser powers and speeds to determine their "onset" and "burning" thresholds, where those for TCDMDA, TCDMDA + HBpPEGDA, HBpTCDMDA, PEGDA, PEGDA + TCDMDA and HBpPEGDA, are shown in Fig. 1.

The results in Fig. 1a demonstrated that the addition of HBpTCDMDA gave a significantly larger operating window compared to when processing with TCDMDA monomer alone. Using the HB polymer positively influenced both the "onset" threshold (reducing the laser power required) and burning threshold (increasing the laser power needed). Both effects were attributed the HB molecular structure, as it acts as a molecularly mobile, "pre-polymerised" network with a high functional group density. Therefore, the HB polymer allows faster cross-linking compared to non-branched "pre-polymers" and less reaction is required comparative to 100% monomer resins, so exotherm generation will be reduced. This is additionally important because using lower laser power allows 2PP printing with smaller voxel sizes to be achieved, potentially leading to better resolution during manufacturing. Furthermore, as it also enables manufacturing structures with higher laser powers before "burning" occurs, so it may also allow structures to be produced at faster processing speeds and with higher cure levels.

By comparison, whilst PEGDA monomer could be printed using the applied conditions, the HBpPEGDA alone formulation exhibited a level of reactivity so high that it did not allow its processing parameters to be determined. The resin was found to auto-polymerise and reach its gel-point before the printing process was completed, so to try to overcome this, different photo-initiator loadings were investigated, but all these resins still gelled. It was hypothesised that diluting the HBpPEGDA could slow its reactivity and gelation, so the material was mixed with TCDMDA to determine if this allowed successful 2PP processing. This mixture also represented a multi-material 2PP printing resin, *i.e.* a hydrophilic/hydrophobic mix. As shown in Fig. 1a, adding 30 wt% of HBpPEGDA to TCDMDA monomer, not only allowed HBpPEGDA to be printed, but also

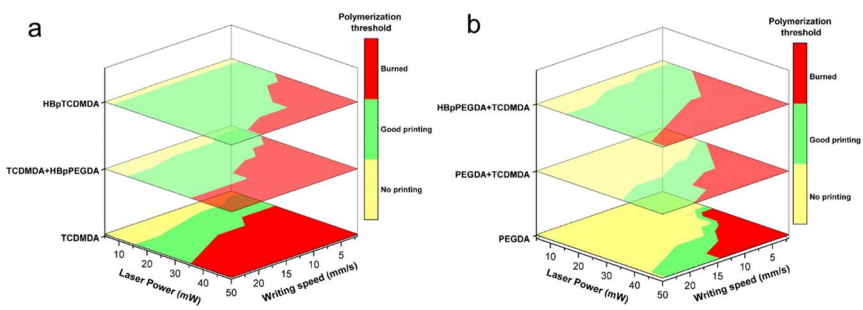

Fig. 1 Map of the screening polymerisation to determine the 2PP thresholds for (a) top to bottom: 100 wt% HBpTCDMDA, TCDMDA 70 wt% + HBpPEGDA 30 wt% and TCDMDA 100 wt%. (b) (top to bottom): HBpPEGDA 50 wt% + TCDMDA 50 wt%, PEGDA 50 wt% + TCDMDA 50 wt% and PEGDA 100 wt% printed using 2 wt% of photoinitiator.

expanded the processing window compared to printing TCDMDA only, improving both the "onset" and "burning" thresholds.

To understand further the 2PP processing of HBpPEGDA, the thresholds of PEGDA alone, PEGDA 50 wt% + TCDMDA 50 wt% and HBpPEGDA 50 wt% + TCDMDA 50 wt% were compared (Fig. 1b). The results showed that, when adding materials to TCDMDA to create a resin, including HBpPEGDA had a more significant impact on the printing parameters than PEGDA. Again, HB polymer addition improved the "onset" threshold, when compared to the other two formulations. This was attributed to the higher reactivity of HBpPEGDA, its flexibility may require less energy density to quickly manufacture an extended network, thus lowering the "onset". However, HBpPEGDA addition lowered the "burning" threshold, so to understand this observation, the thermal decomposition properties of an HB structure were investigated. Thus, a HB polymer of poly(methyl methacrylate) (PMMA), a material that has had its polymerisation/depolymerisation properties extensively studied, was synthesised and subjected to TGA analysis and high temperature degradation.[35–39] This was conducted to explore the potential mechanisms that play a part in the "burning" process, which typically results in the generation of damaged and discoloured builds. These experiments were designed to probe how this part of the printing operational windows is affected by introducing HB polymers into resins, by attempting to mimic the thermal conditions that result from applying high laser powers.

In recent years HB polymers have been used in inkjet printing, where it was reported that including the HB polymers into the resins did not excessively affect the rheological properties of the resins but did improve the curing process at the final curing steps.[26,29,41] The 2PP process in this study involved depositing immersion oil onto a pretreated, silanised glass coverslip, which was then inverted to allow neat resin to be applied to the opposite side. Furthermore, the prepared glass plate was then tilted by up to 15° upon insertion into the holder within the equipment. Thus, the resin was required to be sufficiently viscous to prevent it from spreading beyond the edge of coverslip. Therefore, the in-use viscosity of the resin was interrogated *via* the use of the microscope within the apparatus as part of the printing process. Real time observation of the coverslip *via* this integrated optical microscope with a camera demonstrated that resins consisting of only monomers exhibited the lowest viscosities, such that they were more difficult to mount without spreading on the coverslip. By comparison, the viscosity of the HB included resins was observed to be sufficient to allow stable deposition on the glass coverslip substrate, but that it remained stationary under the optical microscope, with no floating or spreading observed.

Two HBpMMA-*co*-EGDMA HB polymers were synthesised *via* the addition of a crosslinking species (EGDMA), these had MMA : EGDMA ratios of (i) 65 : 35 mol % and (ii) 95 : 05 mol%, respectively. The former HB polymer contains a higher level of crosslinking and so is likely to have a higher branch density. GPC characterisation (Table 1, entries 3 and 4, and Fig. S3) showed that the use of the PhCoBF had produced HB polymers with M_w's similar to that of HBpTCDMDA Meanwhile, the cast-cell products are very high molecular weight materials with a very small level of crosslinker in their formulations, typically <0.5 mol%, suggesting that it is only very slightly branched and would be more like the branched materials that can be produced by the "Strathclyde methodology".[42–44] A schematic of this HB polymer process in shown in Fig. 2a.

Fig. 2b displays images of the reactor vessel after thermal treatment. Fig. 2b(i) clearly shows that the low M_w thermoplastic PMMA completely degrades to leave essentially no discolouration. Meanwhile, both the cell-cast and HB materials did leave residual, discoloured, "charred" material post treatment to 450 °C, Fig. 2b(ii) and (iv), respectively. However, the mass of this residual material is greater in volume with the HB sample (0.53% for Fig. 2b(ii) compared to 26% for Fig. 2b(iv)). When heated to 700 °C, even the lightly crosslinked cell cast materials

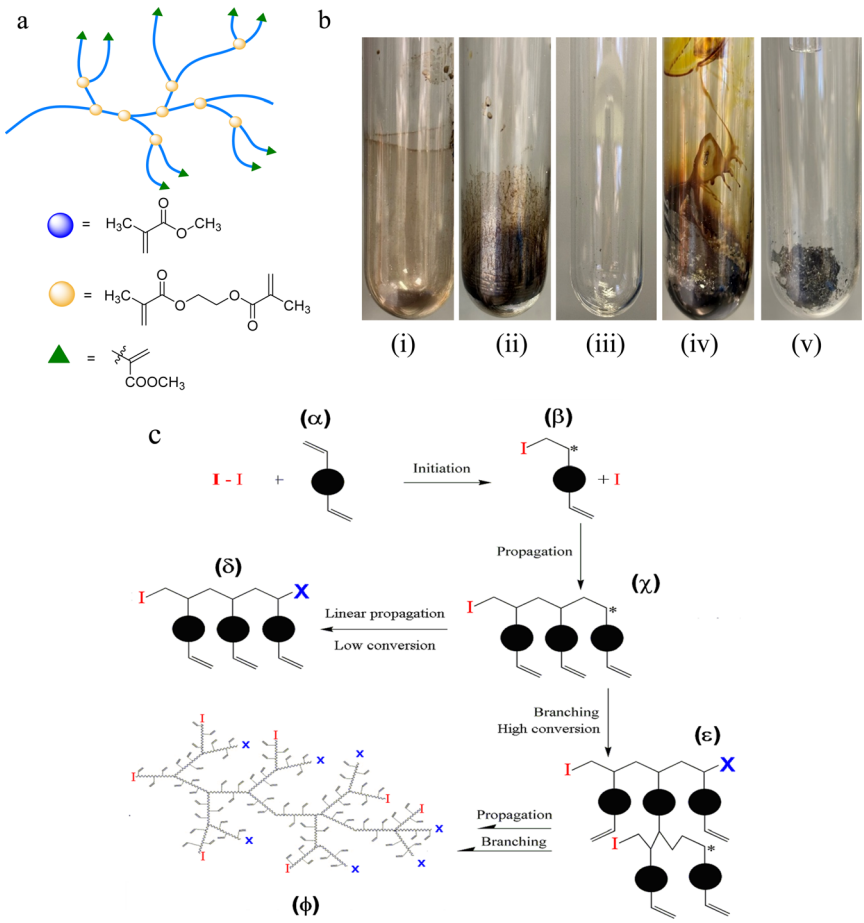

Fig. 2 (a) Schematic of the monomers used to synthesise HBpMMA-*co*-EGDMA which indicates where these monomers locate in the HB structure, (b) presents the results of the degradation of PMMA based polymer where (i) is a commercially purchased PMMA of M_w 15 000 g mol^{-1}, (ii) and (iii) are of commercial cell cast material heated to 450 °C and 700 °C respectively, (iv) and (v) are HBpMMA-*co*-EGDMA polymers with an MMA : EGDMA ratio of 65 : 35% heated to 450 °C and 700 °C respectively and (c) general scheme of the hyperbranching process showing a general initiation species (I) and terminating species (X); (α) initiation of a general difunctional vinyl monomer structure, (β) shows the initiated chain, (χ) propagation of the chain at low conversions to produce polymerising linear functional material, (δ) termination of a portion of this linear functional material, (ε) higher conversion branching reactions and (ϕ) schematic of final HB structure showing presence of initiation and termination end-groups in the final HB structure.

left no residual material, but the HB material left a significant mass of "charred" carbonaceous matter. This clearly indicated that polymerization of crosslinked material could lead to the discolouration observed in 2PP above the "burning" threshold.

The TGA analysis (Fig. S4) confirmed that the HB polymers had a different degradation pathway compared to cast-cell and that the extent of this change was dependent on the level of crosslinking present. Cell-cast (<0.5 mol% crosslinker) material degraded completely, while the HB polymer with 5 mol% crosslinker exhibited a change in mass loss rate at ~10% mass remaining, and the 35 mol% had this change at ~20% residual mass. This indicated that increased crosslinker levels did change the degradation behaviours of HB methacrylate polymers, leading to the presence of residual mass. This data confirmed the degradation data, highlighting that HB polymers have a greater propensity to depolymerise to produce carbonaceous "char" materials, which would explain the decolouration observed in the "burning" zone. Furthermore, the formation of this "char" will probably lead to a greater absorption of energy from the UV lamp due to the colouration, so exacerbating the overheating phenomena that results in the print failure. Furthermore, it also supported the hypothesis that the increased "burning" zone with HBpPEGDA, was related to its greater reactivity, as it reached the onset of this charring/depolymerisation process at lower laser powers, where this effect increases with the increased level of HB content in the resin.

Unfortunately, the concentration at which the HB polymers could be dissolved into solvent resulted in GPC samples that were too weak to obtain an alpha value with an acceptable level of accuracy. Rather, DOSY NMR was conducted on both the HB polymers that were used to compare the depolymerisation performance to polymer structure. It was utilised to define and compare the apparent coil size and branch density for these polymers and this data is shown in Table 3, and Fig. S5 and S6.

The data in Table 3 shows that there is a reduction in the apparent coil size and increase in branching density as the crosslinker level is increased, which suggested that as the crosslinker levels increased the overall globular size of the polymer decreased. This was attributed to the molecular structure being more tightly constrained by the additional branching and that the linear chain sections between the branch points were reducing in length. This DOSY predicted reduced HB globular size also correlated well with the GPC data (Table 2, entries 3 and 4), which recorded a reduction in the molecular weight as the crosslinker level is increased. This suggesting that the GPC data exhibits a strong relationship between the global structure and its hydrodynamic volume. The key processing

Table 3 DOSY NMR data for the MMA : EGDMA 65 : 35 and 95 : 05 mol% HB polymers used in the depolymerisation experimentation

Entry	HBpMMA-*co*-EGDMA co-monomer ratio (mol%)	Apparent coil size[a] (nm)	Branching density
1	95 : 05	3.86	0.025
2	65 : 35	2.20	0.262

[a] Coil radius is calculated from 3.6 ppm ^{1}H NMR peak in $CDCl_3$. This was the largest peak of the polymer repeat unit thus most representative of coil dimensions.

point that this data highlighted was that the level of branching achieved does dictate the level of residual materials that was obtained from the depolymerisation process. Both of these HB polymers produced different residual polymer levels (see TGA data in Fig. S4), where the MMA : EGDMA 65 : 35 sample produces more residual material that the 95 : 05 mol% variant, which was related to the DOSY observation that the latter's branching density is an order of magnitude lower. This also supported the proposal that the cell-cast depolymerisation materials produced char only in the final stages of the depolymerisation process because this is related to an increased concentration of branched species being left in the samples as the depolymerisation process progresses.

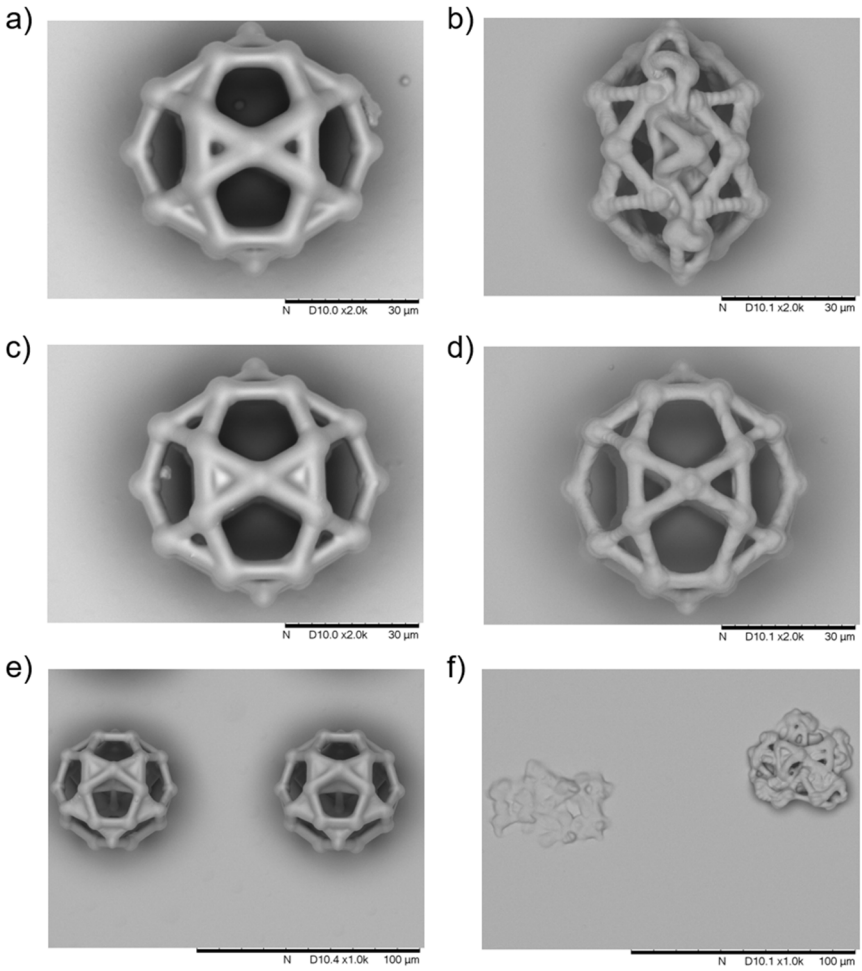

Fig. 3 2PP manufactured buckyball structures produced using 2 wt% initiator with the following mixed monomer resins and processing conditions: (a) HBpPEGDA 50 wt% + TCDMDA 50 wt% and (b) PEGDA 50 wt% + TCDMDA 50 wt% both at laser power 30 mW and 6 mm s^{-1} writing speed; (c) HBpPEGDA 50 wt% + TCDMDA 50 wt% and (d) PEGDA 50 wt% + TCDMDA 50 wt% both at 30 mW and 4 mm s^{-1} speed; (e) HBpPEGDA 50 wt% + TCDMDA 50 wt% and (f) PEGDA 50 wt% + TCDMDA 50 wt% both at 25 mW (left) and 30 mW (right) at 8 mm s^{-1} speed.

To study directly the effect of HB polymers on printing quality and resolution, PEGDA, which is widely used in AM studies, was replaced with HBpPEGDA in a resin formulation, as this would be of broad interest to many 2PP users. So HBpPEGDA 50 wt% + TCDMDA 50 wt% and PEGDA 50 wt% + TCDMDA 50 wt% multi-material resins were formulated and used to fabricate buckyball structures when applying identical printing parameters. The SEM analysis is shown in Fig. 3.

The SEM images showed that replacing PEGDA with HBpPEGDA in a multi-material resin with TCDMDA allowed the successful manufacture of articles that exhibited a smooth surface and structural integrity when using all the printing conditions applied (Fig. 3a, c and 3e). Comparative structures printed with PEGDA + TCDMDA resins with the same set of printing parameters only produced a stable structure at the highest energy print conditions, *i.e.* 30 mW and 4 mm s^{-1} speed (Fig. 3d). The monomer only resin structures processed with less intense energy input (Fig. 3a and e), *i.e.* lower laser power or increased writing speed, were found to collapse. These observations demonstrated that the addition of HB pre-polymer could increase the processing window, as the screening results had suggested. It was proposed that, when using the HB multi-material resins, crosslinking was achieved sufficiently quickly and to an adequate level to produce structures with mechanical properties suitable for the build to be stable with all printing conditions. By comparison, the monomer-based resins were less 2PP compatible because they were only able to deliver these crosslinking thresholds at higher energy conditions. Furthermore, these prints confirmed that HB polymers are suitable for use in Vat AM/2PP because, by reduced the polymerisation "onset" threshold, they allowed the manufacture of structures with good resolution at faster printing speeds. However, printing the more reactive HBpPEGDA resins at the highest power parameters (30 mW and 4 mm s^{-1}) may have led to some overcuring (Fig. 3c and d), such that some gaps in the buckyball have been closed. This also suggested that the higher reactivity of HBpPEGDA may present issues at higher laser powers with a loss of resolution occurring prior to the "burning" onset.

Furthermore, the HBpPEGDA and TCDMDA monomer prints represent a successful multi-material print of complex structures fabricated from two materials of different macro functionality, *i.e.* hydrophilic (HBpPEGDA) and hydrophobic (TCDMDA). Thus, one further potential explanation for the lack of success in printing the monomeric PEGDA and TCDMDA resin is that there may be monomeric microphase separation occurring in the resin. This could result in curing of one monomer and not of the other, based on their relative reactivities and/or the potential phase separation of the photo-initiator into one of the monomer domains only. If the former then, based on the reactivities observed in this paper, it is likely that PEGDA would be the monomer that would preferentially react. Meanwhile, such initiator phase separation has already been reported by the author in inkjet printing.[45] In either case, the result would be 2PP producing only a partially cured print, *i.e.* polymer in unreacted monomer, which is unlikely to hold its shape and would need higher power parameters to overcome these issues. The use of HB polymers in resin formulation may allow 2PP to overcome the incompatibilities of certain monomer types.

Thus, because one moiety was present as a pre-reacted HB polymer and the other was a monomer, the total cure level of all species in the build had to be evaluated. Build quality and cytotoxicity of a printed structure would not remain

constant if significant quantities of unreacted monomer remained. Consequently, 50 μm cubes were fabricated using 50 : 50 wt% TCDMDA + PEGDA, 50 : 50 wt% TCDMDA + HBpPEGDA and 100% PEGDA resin formulations using the printing parameters that successfully produced the buckyballs. These were subjected to analysis by Raman spectroscopy to determine the level of reacted vinyl groups (RVG) in the total structure after printing, so estimating the level of curing obtained. The RVG was calculated by applying eqn (2), as defined in the experimental section. All the spectra demonstrated a decrease in the C=C band peak area after polymerisation compared to that the C=O peak, as this moiety does not participate in the reaction, see Table S3 and spectra in Fig. S5 and S6. Comparison of the RVG values for these printed samples showed no significant differences between them, with all the prints exhibiting a RVG level in the 67 to 71% range. This indicated that adding HBpPEGDA, instead of PEGDA monomer to TCDMDA mixtures does not influence the number of acrylate groups reacted. Hence, it was concluded that, no matter how the branching network is produced, the cure/branching level in all cases reached a point where the structures do not allow the acrylate groups sufficient degrees of freedom of motion to continue to react, as it cannot find another double bond to interact with. Thus, it was proposed the equivalent RVG levels in all these samples meant that the presence of the residual vinyl groups was due to the crosslinking stalling due to the reactions being depleted of molecularly mobile monomer.

The presence of both HBpPEGDA and TCDMDA in this multi-material hydrophobic/hydrophilic 2PP print was then confirmed by ToF-SIMS analysis, where their characteristic ions were observed both on the top surface and in a depth profiling experiment (Fig. 4).

The previously reported characteristic ions associated with HBpPEGDA (43 amu) and pTCDMDA (67 amu) were detected in the cube both at its surface and throughout the first few μm of layers,[46,47] The intensity of HBpPEGDA ions being relatively stronger at the surface than those of TCDMDA due to a higher concentration of ethylene oxide (EO) moles present in the formulation because

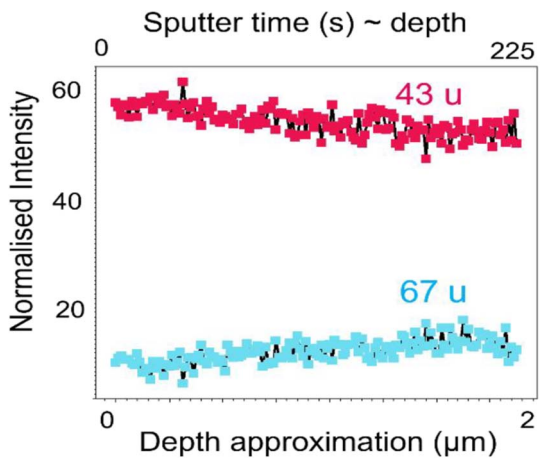

Fig. 4 Normalised intensity of HBpPEGDA ($C_2H_3O^+$/43 amu/red) and TCDMDA ($C_5H_7^+$/67 amu/blue) ions obtained from depth profile analysis.

PEGDA is a polymer. These results indicated that multi-material printing with HB polymers was not only possible, but that good quality multi-materials printed articles could be manufactured with HB : monomer mixed material resin formulations.

Conclusions

This work has focused on evaluating the use of hyperbranched (HB) polymers as novel materials for 2PP processing and to optimise their used in formulating mono- and multi-material two photon polymerisation (2PP) printing resins. This study has shown that the HB materials can be successfully printed in multi-material formulations, where ToF-SIMS analysis on samples manufactured with HBpPEGDA and TCDMDA monomer have confirmed the presence of both materials in the final printed structure. The materials printed represent a multi-functional print, *i.e.* one monomer/polymer is hydrophobic and the other hydrophilic, so the use of HB polymers was demonstrated to aid in the production of such multi-functional structures. It was proposed that this was related to overcoming any mixing disparity in a resin with multi-functional components. Moreover, this study also showed that the use of HB polymers in resins can more broadly extend the range of materials that are available for 2PP processing and can also overcome key polymerisation chemistry restrictions placed on 2PP printing. This both broadens the range of processing conditions that can be applied to successfully produce good quality structures and will allow pre-polymers of monomers that do not react with sufficient speed to be 2PP polymerised as monomers to be included in prints. This influence was attributed to a combination of the HB polymers "globular" structure delivering lower resin viscosities and their relatively high reactive group density compared to that of linear polymers. Hence, when processing with HBpTCDMDA both the polymerisation "onset" and "burning" thresholds were improved compared to those of monomeric resins, *i.e.* lowered and raised respectively. The former was attributed to their high reactive group density, whilst the latter was attributed to the reduction in polymerisation induced exotherm because there is less reaction needed to complete the cure. However, the full impact of the HB polymer type on the printing conditions was shown to be dependent upon the HB polymer's reactivity. When processing HBpPEGDA it was found that, while the overall processing window was increased, the "burning" threshold was in fact lowered. This was proposed to be linked to its greater reactivity, which meant that as polymerisation processes occur more rapidly, so do depolymerisation events. Hence, a HBpMMA-*co*-EGDMA polymer was synthesised and subject to degradation studies. These experiments showed that HB polymers produced more residual material ("char") when subject to high temperature processing than linear materials of the same monomer. Furthermore, comparing the TGA and DOSY NMR data demonstrated that the level of residual material obtained during depolymerisation could be linked to the branching level that the materials exhibited, where increased branching led to increased residual levels. These observations point to the fact that there is more to the burning effect than just the boiling of monomer and it is highly likely that branched polymer degradation is also occurring and causing colourisation. These results show that is it highly important to understand the relative reactivity and homogeneity of printing resin

components if the optimum printing result is to be achieved. Furthermore, when printing complex structures this meant that high quality articles could be produced with lower laser powers and increased writing speeds, giving the opportunity to increase the manufacturing rate from 2PP polymerisation, which is a further step forward for 2PP processing.

Author contributions

AAK, MD, JS, VCC, AS and SG: methodology, validation, investigation, data curation, writing – original draft and review & editing, visualization. GFT: methodology, data curation of ToF-SIMS, writing – review & editing. TS: methodology, data curation of DOSY NMR, writing – review & editing. YH: conceptualization, methodology of 3D printing, writing – review & editing. MA and EB: conceptualization, methodology of microwave processing, writing – review & editing. LRC, CA, RDW and DJI: conceptualization, methodology, writing – review & editing, supervision, project administration, funding acquisition.

Conflicts of interest

There are no conflicts to declare.

Data availability

The data supporting the findings of this study are included in the supplementary information. Access to some of the broader associated data will be restricted until an Intellectual Property filing has been made.

Supplementary information is available. See DOI: **https://doi.org/10.1039/d5fd00097a**.

Acknowledgements

The authors would like to thank the EPSRC for funding this project *via*: (a) the "Formulation for 3D printing: Creating a plug and play platform for a disruptive UK industry grant" (EP/N024818/1) and (b) the Decarbonising The Acrylic Value Chain *via* Resource Circularity prosperity partnership grant jointly funded by the Mitsubishi Chemical Co (UK) Ltd (EP/V038052/1).

References

1 S. Saleh Alghamdi, S. John, N. Roy Choudhury and N. K. Dutta, Additive Manufacturing of Polymer Materials: Progress, Promise and Challenges, *Polymers*, 2021, **13**(5), 753, DOI: **10.3390/polym13050753**.

2 M. Molitch-Hou, 1 - Overview of Additive Manufacturing Process, in *Additive Manufacturing*, ed. J. Zhang and Y.-G. Jung, Butterworth-Heinemann, 2018, pp 1–38, DOI: **10.1016/B978-0-12-812155-9.00001-3**.

3 M. Topa-Skwarczyńska, W. Wałczyk, F. Petko, A. Świeży, W. Wielgus, P. Środa, M. Tyszka-Czochara, K. Trembecka-Wójciga, M. Galek and J. Ortyl, Increasing Resolution in Additive Manufacturing by Using High-Performance and Non-

Toxic Photoinitiating Systems, *Addit. Manuf.*, 2024, **94**, 104473, DOI: **10.1016/j.addma.2024.104473**.

4 A. Stiles, T.-A. Tison, L. Pruitt and U. Vaidya, Photoinitiator Selection and Concentration in Photopolymer Formulations towards Large-Format Additive Manufacturing, *Polymers*, 2022, **14**(13), 2708, DOI: **10.3390/polym14132708**.

5 L. Zhou, J. Miller, J. Vezza, M. Mayster, M. Raffay, Q. Justice, Z. Al Tamimi, G. Hansotte, L. D. Sunkara and J. Bernat, Additive Manufacturing: A Comprehensive Review, *Sensors*, 2024, **24**(9), 2668, DOI: **10.3390/s24092668**.

6 A. Bagheri and J. Jin, Photopolymerization in 3D Printing, *ACS Appl. Polym. Mater.*, 2019, **1**(4), 593–611, DOI: **10.1021/acsapm.8b00165**.

7 A. Zennifer, S. Manivannan, S. Sethuraman, S. G. Kumbar and D. Sundaramurthi, 3D Bioprinting and Photocrosslinking: Emerging Strategies & Future Perspectives, *Biomater. Adv.*, 2022, **134**, 112576, DOI: **10.1016/j.msec.2021.112576**.

8 X. Zhou, Y. Hou and J. Lin, A Review on the Processing Accuracy of Two-Photon Polymerization, *AIP Adv.*, 2015, **5**(3), 030701, DOI: **10.1063/1.4916886**.

9 S. O'Halloran, A. Pandit, A. Heise and A. Kellett, Two-Photon Polymerization: Fundamentals, Materials, and Chemical Modification Strategies, *Adv. Sci.*, 2023, **10**(7), 2204072, DOI: **10.1002/advs.202204072**.

10 K. Stokes, K. Clark, D. Odetade, M. Hardy and P. Goldberg Oppenheimer, Advances in Lithographic Techniques for Precision Nanostructure Fabrication in Biomedical Applications, *Discover Nano*, 2023, **18**(1), 153, DOI: **10.1186/s11671-023-03938-x**.

11 Y. Liu, X. He, C. Yuan, P. Cao and X. Bai, Antifouling Applications and Fabrications of Biomimetic Micro-Structured Surfaces: A Review, *J. Adv. Res.*, 2024, **59**, 201–221, DOI: **10.1016/j.jare.2023.08.019**.

12 M. Carlotti and V. Mattoli, Functional Materials for Two-Photon Polymerization in Microfabrication, *Small*, 2019, **15**(40), 1902687, DOI: **10.1002/smll.201902687**.

13 Q. Hu, X.-Z. Sun, C. D. J. Parmenter, M. W. Fay, E. F. Smith, G. A. Rance, Y. He, F. Zhang, Y. Liu, D. Irvine, C. Tuck, R. Hague and R. Wildman, Additive Manufacture of Complex 3D Au-Containing Nanocomposites by Simultaneous Two-Photon Polymerisation and Photoreduction, *Sci. Rep.*, 2017, **7**(1), 17150, DOI: **10.1038/s41598-017-17391-1**.

14 S. K. Saha, B. Au and J. S. Oakdale, High-Speed Direct Laser Writing of Silver Nanostructures via Two-Photon Reduction, *Adv. Eng. Mater.*, 2019, **21**(9), 1900583, DOI: **10.1002/adem.201900583**.

15 B. Buchegger, C. Vidal, J. Neuwirth, B. Buchroithner, A. Karner, A. Hochreiner, T. A. Klar and J. Jacak, Gold Nanoislands Grown on Multiphoton Polymerized Structures as Substrate for Enzymatic Reactions, *ACS Mater. Lett.*, 2019, **1**(4), 399–403, DOI: **10.1021/acsmaterialslett.9b00182**.

16 V. Harinarayana and Y. C. Shin, Two-Photon Lithography for Three-Dimensional Fabrication in Micro/Nanoscale Regime: A Comprehensive Review, *Opt. Laser Technol.*, 2021, **142**, 107180, DOI: **10.1016/j.optlastec.2021.107180**.

17 F. Franco-Martínez, C. Grasl, E. Kornfellner, M. Vostatek, A. M. Cendrero, F. Moscato and A. D. Lantada, Hybrid Design and Prototyping of

Metamaterials and Metasurfaces, *Virtual Phys. Prototyp.*, 2022, **17**, 1031–1046, DOI: **10.1080/17452759.2022.2101009**.

18 Z. Faraji Rad, P. D. Prewett and G. J. Davies, High-Resolution Two-Photon Polymerization: The Most Versatile Technique for the Fabrication of Microneedle Arrays, *Microsyst. Nanoeng.*, 2021, **7**(1), 71, DOI: **10.1038/s41378-021-00298-3**.

19 Q. Hu, G. A. Rance, G. F. Trindade, D. Pervan, L. Jiang, A. Foerster, L. Turyanska, C. Tuck, D. J. Irvine, R. Hague and R. D. Wildman, The Influence of Printing Parameters on Multi-Material Two-Photon Polymerisation Based Micro Additive Manufacturing, *Addit. Manuf.*, 2022, **51**, 102575, DOI: **10.1016/j.addma.2021.102575**.

20 A. Jaiswal, C. K. Rastogi, S. Rani, G. P. Singh, S. Saxena and S. Shukla, Two Decades of Two-Photon Lithography: Materials Science Perspective for Additive Manufacturing of 2D/3D Nano-Microstructures, *iScience*, 2023, **26**(4), 106374, DOI: **10.1016/j.isci.2023.106374**.

21 T. Zandrini, N. Liaros, L. J. Jiang, Y. F. Lu, J. T. Fourkas, R. Osellame and T. Baldacchini, Effect of the Resin Viscosity on the Writing Properties of Two-Photon Polymerization, *Opt. Mater. Express*, 2019, **9**(6), 2601–2616, DOI: **10.1364/OME.9.002601**.

22 A. Foerster, V. Annarasa, A. Terry, R. Wildman, R. Hague, D. Irvine, D. S. A. De Focatiis and C. Tuck, UV-Curable Silicone Materials with Tuneable Mechanical Properties for 3D Printing, *Mater. Des.*, 2021, **205**, 109681, DOI: **10.1016/j.matdes.2021.109681**.

23 R. J. Mondschein, A. Kanitkar, C. B. Williams, S. S. Verbridge and T. E. Long, Polymer Structure-Property Requirements for Stereolithographic 3D Printing of Soft Tissue Engineering Scaffolds, *Biomaterials*, 2017, **140**, 170–188, DOI: **10.1016/j.biomaterials.2017.06.005**.

24 S. R. Goodwin, A. Stimpson, R. Moon, L. Cowie, N. Aragrag, S. V. Filip, A. G. Smith and D. J. Irvine, Facile Synthesis of Functionalised Hyperbranched Polymers for Application as Novel, Low Viscosity Lubricant Formulation Components, *Polymers*, 2022, **14**(18), 3841, DOI: **10.3390/polym14183841**.

25 C.-J. Chang, Y.-H. Lin and H.-Y. Tsai, Synthesis and Properties of UV-Curable Hyperbranched Polymers for Ink-Jet Printing of Color Micropatterns on Glass, *Thin Solid Films*, 2011, **519**(15), 5243–5248, DOI: **10.1016/j.tsf.2011.01.168**.

26 H. Xiang, X. Wang, G. Lin, L. Xi, Y. Yang, D. Lei, H. Dong, J. Su, Y. Cui and X. Liu, Preparation, Characterization and Application of UV-Curable Flexible Hyperbranched Polyurethane Acrylate, *Polymers*, 2017, **9**(11), 552, DOI: **10.3390/polym9110552**.

27 J. S. R. Wheeler, A. Longpré, D. Sells, D. McManus, S. Lancaster, S. W. Reynolds and S. G. Yeates, Effect of Polymer Branching on Degradation during Inkjet Printing, *Polym. Degrad. Stab.*, 2016, **128**, 1–7, DOI: **10.1016/j.polymdegradstab.2016.02.012**.

28 Y. Hao, J. Gao, Z. Xu, N. Zhang, J. Luo and X. Liu, Preparation of Silver Nanoparticles with Hyperbranched Polymers as a Stabilizer for Inkjet Printing of Flexible Circuits, *New J. Chem.*, 2019, **43**(6), 2797–2803, DOI: **10.1039/C8NJ05639K**.

29 S. Jafarifard, S. Bastani, A. Soleimani-Gorgani and M. G. Sari, The Chemo-Rheological Behavior of an Acrylic Based UV-Curable Inkjet Ink: Effect of

Surface Chemistry for Hyperbranched Polymers, *Prog. Org. Coat.*, 2016, **90**, 399–406, DOI: **10.1016/j.porgcoat.2015.08.007**.

30 Y. Zheng, S. Li, Z. Weng and C. Gao, Hyperbranched Polymers: Advances from Synthesis to Applications, *Chem. Soc. Rev.*, 2015, **44**(12), 4091–4130, DOI: **10.1039/C4CS00528G**.

31 B. Mu, T. Liu and W. Tian, Long-Chain Hyperbranched Polymers: Synthesis, Properties, and Applications, *Macromol. Rapid Commun.*, 2019, **40**(17), 1970042, DOI: **10.1002/marc.201970042**.

32 T. Cuneo and H. Gao, Recent Advances on Synthesis and Biomaterials Applications of Hyperbranched Polymers, *Wiley Interdiscip. Rev.: Nanomed.*, 2020, **12**(6), e1640, DOI: **10.1002/wnan.1640**.

33 L. Ning, J. Chen, J. Sun, Y. Liu, D. Yi and J. Cao, Preparation and Properties of 3D Printing Light-Curable Resin Modified with Hyperbranched Polysiloxane, *ACS Omega*, 2021, **6**(37), 23683–23690, DOI: **10.1021/acsomega.1c01232**.

34 M. P. Seah, Universal Equation for Argon Gas Cluster Sputtering Yields, *J. Phys. Chem. C*, 2013, **117**(24), 12622–12632, DOI: **10.1021/jp402684c**.

35 E. K. C. Moens, K. De Smit, Y. W. Marien, A. D. Trigilio, P. H. M. Van Steenberge, K. M. Van Geem, J.-L. Dubois and D. R. D'hooge, Progress in Reaction Mechanisms and Reactor Technologies for Thermochemical Recycling of Poly(Methyl Methacrylate), *Polymers*, 2020, **12**(8), 1667, DOI: **10.3390/polym12081667**.

36 C. D. Borman, A. T. Jackson, A. Bunn, A. L. Cutter and D. J. Irvine, Evidence for the Low Thermal Stability of Poly(Methyl Methacrylate) Polymer Produced by Atom Transfer Radical Polymerisation, *Polymer*, 2000, **41**(15), 6015–6020, DOI: **10.1016/S0032-3861(00)00020-3**.

37 Y.-H. Hu and C.-Y. Chen, The Effect of End Groups on the Thermal Degradation of Poly(Methyl Methacrylate), *Polym. Degrad. Stab.*, 2003, **82**(1), 81–88, DOI: **10.1016/S0141-3910(03)00165-4**.

38 B. J. Holland and J. N. Hay, The Effect of Polymerisation Conditions on the Kinetics and Mechanisms of Thermal Degradation of PMMA, *Polym. Degrad. Stab.*, 2002, **77**(3), 435–439, DOI: **10.1016/S0141-3910(02)00100-3**.

39 T. Kashiwagi, A. Inaba, J. E. Brown, K. Hatada, T. Kitayama and E. Masuda, Effects of Weak Linkages on the Thermal and Oxidative Degradation of Poly(Methyl Methacrylates), *Macromolecules*, 1986, **19**(8), 2160–2168, DOI: **10.1021/ma00162a010**.

40 D. M. Haddleton, D. R. Maloney, K. G. Suddaby, A. V. G. Muir and S. N. Richards, Catalytic Chain Transfer Polymerisation (CCTP) of Methyl Methacrylate: Effect of Catalyst Structure and Reaction Conditions on Chain Transfer Coefficient, *Macromol. Symp.*, 1996, **111**(1), 37–46, DOI: **10.1002/masy.19961110106**.

41 J. Han, T. Liu, S. Zhang, C. Hao, J. Xin, B. Guo and J. Zhang, Hyperbranched Polymer Assisted Curing and Repairing of an Epoxy Coating, *Ind. Eng. Chem. Res.*, 2019, **58**(16), 6466–6475, DOI: **10.1021/acs.iecr.9b00800**.

42 N. O'Brien, A. McKee, D. C. Sherrington, A. T. Slark and A. Titterton, Facile, Versatile and Cost Effective Route to Branched Vinyl Polymers, *Polymer*, 2000, **41**(15), 6027–6031, DOI: **10.1016/S0032-3861(00)00016-1**.

43 F. Isaure, P. A. G. Cormack and D. C. Sherrington, Facile Synthesis of Branched Poly(Methyl Methacrylate)s, *J. Mater. Chem.*, 2003, **13**(11), 2701–2710, DOI: **10.1039/B303321J**.

44 G. Saunders, P. A. G. Cormack, S. Graham and D. C. Sherrington, Use of Rapid Triple Detection Size Exclusion Chromatography to Evaluate the Evolution of Molar Mass and Branching Architecture during Free Radical Branching Copolymerization of Methyl Methacrylate and Ethylene Glycol Dimethacrylate, *Macromolecules*, 2005, **38**(15), 6418–6422.

45 L. Ruiz-Cantu, G. F Trindade, V. Taresco, Z. Zhou, Y. He, L. Burroughs, E. A. Clark, F. R. A. J. Rose, C. Tuck, R. Hague, C. J. Roberts, M. Alexander, D. J. Irvine and R. D. Wildman, Bespoke 3D-Printed Polydrug Implants Created via Microstructural Control of Oligomers, *ACS Appl. Mater. Interfaces*, 2021, **13**(33), 38969–38978, DOI: **10.1021/acsami.1c07850**.

46 A. Nasir, J. Thorpe, L. Burroughs, J. Meurs, S. Pijuan-Galito, D. J. Irvine, M. R. Alexander and C. Denning, Discovery of a Novel Polymer for Xeno-Free, Long-Term Culture of Human Pluripotent Stem Cell Expansion, *Adv. Healthcare Mater.*, 2021, **10**(6), 2001448, DOI: **10.1002/adhm.202001448**.

47 M. Dubey, K. Emoto, F. Cheng, L. J. Gamble, H. Takahashi, D. W. Grainger and D. G. Castner, Surface Analysis of Photolithographic Patterns Using ToF-SIMS and PCA, *Surf. Interface Anal.*, 2009, **41**(8), 645–652, DOI: **10.1002/sia.3056**.